Send Orders for Reprints to reprints@benthamscience.net

Mini-Reviews in Medicinal Chemistry, 2021, *21*, 000-000

MINI-REVIEW ARTICLE

Nanomaterials for Deep Tumor Treatment

Daria Yu. Kirsanova[1,*], Zaira M. Gadzhimagomedova[1], Aleksey Yu. Maksimov[2] and Alexander V. Soldatov[1]

[1]*The Smart Materials Research Institute, Southern Federal University, Sladkova 178/24, 344090, Rostov-on-Don, Russia;* [2]*National Medical Research Centre for Oncology, 14 liniya str. 63, 344037, Rostov-on-Don, Russia*

ARTICLE HISTORY

Received: May 19, 2020
Revised: July 25, 2020
Accepted: August 20, 2020

DOI:
10.2174/1389557520666201111161705

Abstract: According to statistics, cancer is the second leading cause of death in the world. Thus, it is important to solve this medical and social problem by developing new effective methods for cancer treatment. An alternative to more well-known approaches, such as radiotherapy and chemotherapy, is photodynamic therapy (PDT), which is limited to the shallow tissue penetration (< 1 cm) of visible light. Since the PDT process can be initiated in deep tissues by X-ray irradiation (X-ray induced PDT, or XPDT), it has a great potential to treat tumors in internal organs. The article discusses the principles of therapies. The main focus is on various nanoparticles used with or without photosensitizers, which allow the conversion of X-ray irradiation into UV-visible light. Much attention is given to the synthesis of nanoparticles and analysis of their characteristics, such as size and spectral features. The results of *in vitro* and *in vivo* experiments are also discussed.

Keywords: X-ray photodynamic therapy, photodynamic therapy, cancer treatment, photosensitizer, nanoparticle, scintillator, nanomaterials, reactive oxygen species.

1. INTRODUCTION

It is known that cancer is one of the most serious and dangerous diseases of our time, while cancer mortality is one of the most socially significant problems worldwide. Moreover, according to the World Health Organization (WHO) database [1], about 1 410 000 cancer deaths in the European Union for 2019 were estimated [2]. Therefore, scientists are trying to develop various techniques to fight this disease. Nowadays, there are a lot of approaches for cancer treatment available, such as surgery, radiotherapy, chemotherapy, immunotherapy, or hormone therapy that can be selected depending on the type and stage of cancer. Unfortunately, some of these therapies demonstrate a low selectivity for cancer cells in the body and often high toxicity to normal cells that can cause serious side effects. Thus, an unconventional approach known as Photodynamic Therapy (PDT) was developed as opposed to the conventional cancer treatments listed above [3, 4]. The main limitation of PDT is the shallow tissue penetration (<1 cm) that can be overcome in deep tissues with X-ray irradiation. There are several review articles on the topic of X-ray photodynamic therapy (XPDT). Some of them are certainly informative and can help scientists interested in this field of science to understand it more precisely [5-7]. Moreover, some of the articles were written several years ago [8-12], or they do not include all information about nanomaterials, which are used in therapy [13, 14]. Thus, the present review article includes more recent information about this topic.

*Address correspondence to this author at the The Smart Materials Research Institute, Southern Federal University, Sladkova 178/24, 344090, Rostov-on-Don, Russia; E-mail: dkirs27@gmail.com

2. PRINCIPLES

2.1. Photodynamic Therapy

Photodynamic therapy is an alternative method of treating cancer, some skin diseases, or infectious diseases based on the use of photosensitive substances (photosensitizers) and light of a certain wavelength.

The principle of therapy includes three main components: photosensitizer (PS), light, and oxygen. The sensitizer is most often injected into the body intravenously, and then it accumulates in a tumor or other target tissues (cells) selectively. After that, the tissues which were affected by the pathological process are irradiated with light of a wavelength corresponding to or close to the maximum absorption of the photosensitizer. Nowadays, laser installations are used as a light source, which can emit light of a certain wavelength with high intensity.

The absorption of photons by the photosensitizer molecules in the presence of oxygen leads to photochemical reactions. When PS absorbs the energy upon irradiation, electrons from the ground state are transformed into a short-lived excited singlet state, which can be converted to the long-lived excited triplet state. Then this excited triplet state of PS can undergo two types of reactions. In the type I mechanism, electron transfers to form radicals that in the presence of

1389-5575/21 $65.00+.00

ambient oxygen cab produce Reactive Oxygen Species (ROS), such as hydrogen peroxide (H_2O_2), hydroxyl radicals (•OH) and oxygen radicals ($•O_2$). Otherwise, in the type II mechanism, the triplet electron directly transfers the energy to triplet oxygen ($^3O_2$) nearby to form highly reactive singlet oxygen ($^1O_2$). Besides, these two reactions can occur simultaneously [5, 15-16].

Even though PDT is a promising method for treating tumors, and it is less invasive compared to other treatment methods such as surgery, radiation therapy, and chemotherapy, but this approach has some limitations. Particularly, PDT is limited to the shallow tissue penetration of visible light, which reduces the efficiency of the destruction of tumors located in deeper tissues. Nevertheless, different approaches have been developed to overcome this difficulty. Some of them use the tissue transparency window in the near-infrared (700-1000 nm); in other words, it is an interval of wavelength where light has its maximum depth of penetration in tissue. The next way to remove the above-mentioned limitations is to use the novel sensitizers, which will be conjugated with luminescent nanoparticles [17-24], nanodots [25], or MOFs [26-30]. Although these approaches improve the penetration depth of exciting light, PDT still has limitations to treating tumors under the skin or on the mucous membrane of some internal organs.

For example, Mokoena *et al.* [31] synthesized Er^{3+} and Yb^{3+} co-doped $Sr_5(PO_4)_3OH$ phosphors powders with a combustion method using urea as a fuel. Then the crystal structure, particle morphology, and upconversion luminescence of this material were analyzed. The XRD and SEM of $Sr_5(PO_4)_3OH:Er^{3+}$, Yb^{3+} showed that the powder was made up of hexagonal nanospheres. Moreover, the schematic energy transfer diagram for Er^{3+}/Yb^{3+} was shown. The enhancement of red emission from Er^{3+} at ~660 nm was demonstrated: Yb^{3+} was used as a sensitizer that gathered primary excitation energy and transferred to $Er^{3+,}$ enhancing its red emission. It is necessary to note that light energy in wavelengths in the range of 600–900 nm (far-red to NIR) can penetrate living tissues to a depth of about 8-10 nm and treat surface wounds, cuts, scars, and cancerous cells. Thus, $Sr_5(PO_4)_3OH:Er^{3+}$, Yb^{3+} phosphors powders can be used in light therapy to activate photosensitizers for photodynamic therapy because of its red-emitting.

Recently, Tavakkoli *et al.* [32] synthesized LaF_3: Ag luminescent nanoparticles (NPs), analyzed them with XRD and SEM, and then chemically conjugated LaF_3: Ag with the photosensitizer protoporphyrin (PpIX) using cysteine as a mediator. Such nanomaterials were chosen because the emission spectrum of LaF_3: Ag NPs and the absorption band of PpIX are mostly overlapped with each other. In this way, these NPs are used as a light source for PDT because they activate PpIX and increase the quantum yield of ROS. It was found that after irradiation with UV light, these NPs have a long-lasted afterglow in a time interval of more than 40 min. This property can help to deliver them without demanding subsequent excitation to the deeply located tumors, exciting the nanocomposites outside the body.

In parallel with the above research, Sengar *et al.* [33] synthesized and characterized YAG:Pr@ZnO@PpIX nanocomposite, which consists of UV-emitting $Y_{2.99}Pr_{0.01}Al_5O_{12}$ (YAG: Pr) nanoscintillator, zinc oxide (ZnO) and PpIX as a photosensitizer. Upon direct and indirect photoactivation with UV_{365nm} and UV_{290nm} this nanohybrid can produce both Type I and Type II ROS, respectively. The preparation of this nanomaterial includes three steps: synthesis of the Pr^{3+}-doped YAG (YAG: Pr) scintillating nanoparticles (ScNPs) by the sol-gel method, then coating a thin layer of semiconductor ZnO on the surface of YAG:Pr by atomic layer deposition to give a core-shell structure YAG:Pr@ZnO, and conjugation of these nanocomposites with PpIX using aminopropyl trimethoxy silane (APTMS) as a linker to form YAG:Pr@ZnO@PpIX. The presence of efficient energy transfer both from YAG: Pr to ZnO (at ~320 nm) and from YAG:Pr@ZnO to PpIX (at 350-450 nm – the so-called Soret region) was determined using photo- and cathodoluminescence analyses. It is necessary to note the fact that without activation YAG:Pr@ZnO@PpIX nanocomposite showed low toxicity in mouse melanoma cells, but upon photoactivation with UV_{365nm}, the cytotoxicity increased significantly.

Another nanomaterial that may be used for PDT is quantum dots (QDs), but the toxicity of such QDs and the low overall efficiency of these hybrids are still problematic. Thus, Charron *et al.* [34] conjugated the photosensitizer chlorin e6 and two types (sizes) of less-toxic InP/ZnS QDs coated with a thin silica layer. The *in vitro* experiments were conducted on the MDA-MB231 breast cancer cell line using these QD/chlorin e6 hybrids. Then cancer cells were irradiated with UV light for 5 min (total irradiation dose 0.033 J/cm^2). The same cell viability was detected for QD/chlorin e6 hybrid (concentration 26 nM) and the free photosensitizer chlorin e6 (concentration 24 nM) alone. This may be because the rate of production of singlet oxygen of the QD/chlorin e6 hybrid was lower compared with the free photosensitizer.

It is already known that carbon nanostructures have a wide variety of promising applications in environmental, energy, and biomedical fields. So, it may lead to a new generation of carbon-based nanomaterial PDT agents. Ge *et al.* [35] found that a new PDT agent based on graphene quantum dots (GQDs) exhibits good biocompatibility and can produce singlet oxygen $^1O_2$ with a quantum yield of ~1.3, which is the highest reported for PDT agents. This extremely high $^1O_2$ quantum yield of the GQDs happens because of a new $^1O_2$-generating mechanism, which can be termed multistate sensitization. The GQDs were synthesized by hydrothermal treatment of polythiophene (PT2) which was used as the carbon source.

2.2. X-ray Photodynamic Therapy

Another alternative approach relies on the use of scintillating nanoparticles that upon exposure to ionizing radiation, such as X-ray, emit luminescence in the visible region, which, in turn, activates a conjugated photosensitizer through Förster resonance energy transfer (FRET) and leads to the generation of reactive oxygen species (Fig. **1**). A step-by-step algorithm of the therapy is presented in Fig. (**2**).

Some photosensitizers can be used alone, even for X-ray irradiation without nanoparticles to treat malignant tumors. For example, molecular modification of protoporphyrin IX

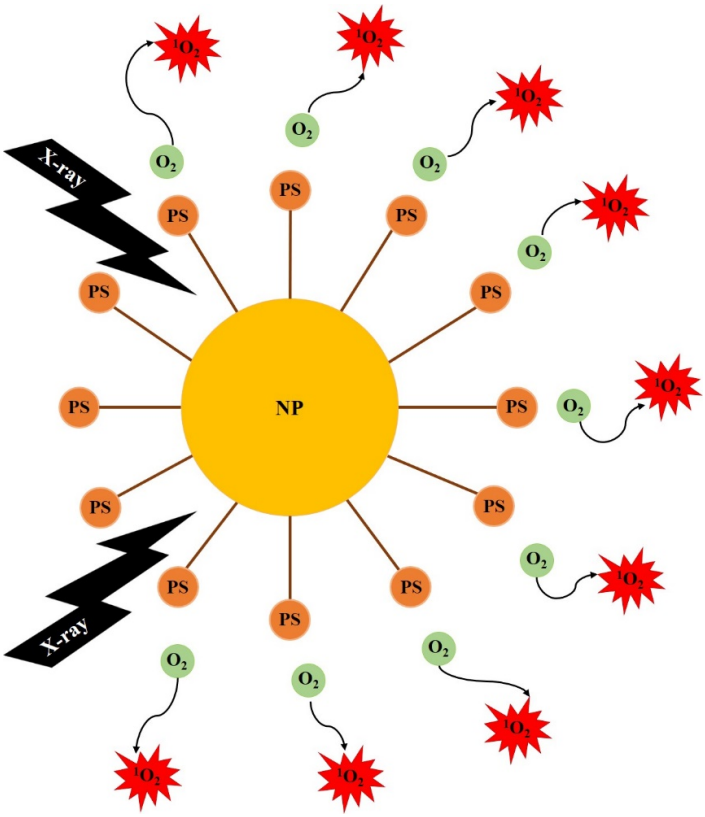

Fig. (1). The mechanism of XPDT (NP – nanoparticle, PS – photosensitizer). *(A higher resolution / colour version of this figure is available in the electronic copy of the article).*

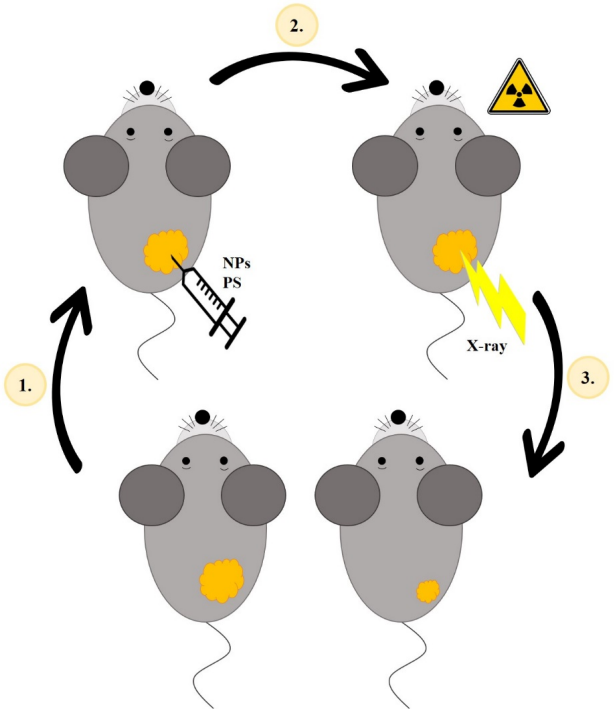

Fig. (2). The scheme of *in vivo* XPDT experiment (NPs – nanoparticles, PS – photosensitizer). *(A higher resolution / colour version of this figure is available in the electronic copy of the article).*

(MPpIX) can be used for deep cancer treatment upon X-ray, which in turn can penetrate deeply into tissue. It was studied by Homayone and co-workers in 2015 [36]. MPpIX was prepared in the following way. Firstly, after conjugation with 3-aminopropyl triethoxysilane (APTES), the carboxylic acid and the two nitrogen atoms in the core of PpIX molecule were protonated. Then, folic acid (FA) and the APTES-coated PpIX (MPpIX) were conjugated due to the chemical bonding between FA and protonated PpIX. The results showed that the coating of APTES on PpIX largely increases its water dispersion, stability, and luminescence efficiency, and under the same conditions, the cell uptake is higher for MPpIX compared to PpIX. As a result, these factors increase the generation of singlet oxygen. Homayone *et al.* detected singlet oxygen in the MPpIX upon X-ray irradiation and used for this purpose the p-nitrosodimethylaniline (RNO)-imidazole (ID) method.

Certainly, nanoparticles that can be selected for conjugation with photosensitizer should follow some requirements. Firstly, the nanoparticles must be easily attached to photosensitizers, stable in biological environments, harmless, and water-soluble. As it was pointed out by Chen *et al.* [37], nanomaterials are promising as potential carriers of photosensitizers because they can be made hydrophilic, they possess relatively large surface areas that can be modified with functional groups, they can penetrate deep into the tissue through fine capillaries and be generally taken up efficiently by cells. In addition, there are currently a lot of methods for producing these nanomaterials. In order to be used as a PDT light source, NPs selected for photosensitizer enhancement must meet the following requirements: the nanoparticle emission spectrum must match the photosensitizer's absorption spectrum. The matching of the nanoparticle emission band with the photosensitizer absorption band makes it possible to efficiently activate the photosensitizers and, as a result, to generate ROS. Moreover, the nanoparticles must have high luminescence efficiency, *i.e.*, excitation by an X-ray beam should result in strong optical emission by the nanoparticle. Finally, the nanoparticles should be close to the photosensitizers and have a large surface area to transfer photon energy.

In addition, it is necessary to conduct a toxicopathological evaluation of tissues to evaluate any risks and identify the hazard of nanoparticles. For this purpose, Ostrowski *et al.* [38] made a comparison of analytical methods for the visualization of nanoparticles in tissues because it is often not enough to use a single technique to solve all the problems related to the cellular uptake or the distribution of nanoparticles within the target cells and tissues. Thus, it can be more beneficial to use a combination of different detection methods that can provide reliable information about histomorphologic changes associated with the biodistribution of nanomaterials in the body. Significantly, a lot of imaging procedures that can be used for localizing NPs in the body do not permit a precise quantitative analysis of the number of NPs in the tissues under study because of the limited resolution of some analytical approaches. But for semiquantitative assessment of the number of NPs in tissues can be obtained using such approaches as a pixel analysis or counting fluorescent spots.

3. X-RAY-INDUCED SENSITIZERS USED IN XPDT

X-ray-induced sensitizers used in XPDT can be divided into several groups, which are outlined below.

3.1. Nanoparticles without Photosensitizers

Recently, other samples, such as europium doped hafnium dioxide NPs, were shown to be perspective for the conversion of direct X-ray to ROS. These HfO_2:Eu nanoparticles were prepared using a microwave hydrothermal route, then structurally and spectroscopically analyzed with different methods (for example, XRD, TEM, SEM, PL), and finally *in vivo* experiments on mouse and rat were conducted by Kaszewski *et al.* [39]. It was determined that the layer on the surface appearing during the crystallization of nanoparticles in the process is responsible for efficient photoluminescence. Moreover, these HfO_2:Eu NPs were found useable in biological imaging of rodents' tissues.

Sapre *et al.* [40] showed that the scintillator nanoparticles of $(Y_{1-x}Pr_x)_3Al_5O_{12}$ (YAG:Pr) with x = 0.01 can be very useful in XPDT because of a very low biological toxicity of yttrium, praseodymium, and aluminum. These nanoparticles were synthesized with a sol-gel synthesis technique, which included the hourly key step of calcination at 1400^{o}C. It should be noted that it was necessary to prepare the smooth spherical YAG:Pr nanoparticles with 10-200 nm in diameter to minimize blood vessel wall damage and to be able to accumulate in tumor *via* the enhanced permeability and retention (EPR) effect. Moreover, it was shown that YAG:Pr nanoparticles can be coated with a thin, functionalizing silica layer, but the photon emission spectra for the uncoated and silica-coated particles are similar, except for the fact that the silica coating acted as a barrier to light transmission reducing the measured peak photon flux by about 25%. Thus, coating YAG:Pr particles with silica will not adversely affect nanoscintillator photon emission, and it may be used for introducing functional groups to the particle surfaces.

Moreover, an efficient scintillator based on $NaYF_4$:Gd nanorods (NRs) doped with different concentrations of terbium ions were synthesized by a facile hydrothermal approach and then applied for optical bioimaging under X-ray irradiation by Li *et al.* [41]. After *in vitro* experiments, optical imaging resulted that the $NaYF_4$:Gd/Tb NRs can efficiently emit green light under X-ray, and it should be noted that the largest emission intensity was determined for sample doped with 15% Tb. The *in vivo* experiments were conducted on samples of pork tissue with different thicknesses that were placed between the $NaYF_4$:40% Gd/15% Tb NRs and the soft X-ray irradiation. The X-ray light source has an operating voltage at 45 kV and the irradiation time is 1 min. It was determined that the maximum penetration depth was estimated to be approximately 6 mm under X-ray excitation (45 kV, 2 min). As for cytotoxicity analysis, the cell viability was above 96% (the concentration of the NRs was 50 μg/mL) and slightly reduced with a further increase in the concentration. However, the cell viability was still maintained around 85%, indicating the low cytotoxicity of NRs even when its concentration was at a relatively high dose of 1000 μg/mL.

A little bit earlier, Sadjadpour *et al.* [42] obtained that ZnO nanoparticles alone exerted cytotoxicity upon X-ray irradiation, making it useful for the treatment of deep cancers. Cytotoxic effects on T-47D and Du145 cell lines were determined for different concentrations of nanoparticles X-ray irradiation (0.94 Gy, 70 kV, and 8 mA). It was determined that concentrations greater than 7.5 μM showed considerable cytotoxic effects with or without X-ray irradiation, while concentrations below 0.75 μM did not show any significant cytotoxicity even under X-ray irradiation. It was also observed that under X-ray irradiation, incubation of T-47D and Du145 cells with ZnO nanoparticles resulted in significant cytotoxic effects, especially at the highest concentration (60 μM). Thus, the viability of T-47D and Du145 cancer cells incubated with ZnO under X-ray irradiation reduced to 20% and 30%, respectively. Sadjadpour *et al.* also conjugated these ZnO NPs with porphyrin photosensitizers (MTCP and CuMTCP) and demonstrated that none of the ZnO-porphyrin conjugates caused hazard effects on cancer cells after activation with X-ray in contrast with ZnO.

At the same time, another group of researchers synthesized scintillating ZnO/SiO_2 core-shell nanoparticles, in which due to the amphoteric properties of ZnO core, Generalov *et al.* [43] coated with a silica layer to ensure chemical stability in a biologically relevant environment. *In vitro* experiments were carried out on two human prostate adenocarcinoma cell lines – LNCaP and Du145. It should be noted that concentrations of the ZnO/SiO_2 nanoparticles were selected so that cell toxicity does not exceed 20%. After incubation, the cells were irradiated with 200 kVp X-ray. Nanoparticles disastrously affect cancer cells and reduce their survival by about 2-fold for LNCaP and 1.5-fold for Du145 cells.

3.2. Nanoparticles with Photosensitizers

It has already been mentioned that the conjugates of nanoparticle and photosensitizer activated with X-ray (Fig. **2**) can be used either to supplement the radiotherapy for cancer treatment or as an independent treatment approach. It was found by Popovich *et al.* [44] that protoporphyrin IX (PpIX) and $CeF_3:Tb^{3+}$-based nanoparticles, which were modified with SiO_2, can be used for studying the luminescent properties of these conjugates. The nanoparticles were synthesized *via* sol-gel methods and then modified with SiO_2 and PpIX. To detect the generation of singlet oxygen, APF commercial probe was used. Besides XRD and TEM analyses, radioluminescence (RL) and photoluminescence (PL) emission spectra were measured using the X-ray tube to evaluate the luminescence characteristics of the material. Particularly, an energy transfer from Ce^{3+} to Tb^{3+} ions and from Tb^{3+} to PS molecules was proven *via* RL analysis. Thus, studied conjugates may be good candidates for the application in XPDT.

Ma *et al.* [45] showed that X-ray irradiation can be used to excite conjugates of ZnS:Cu,Co afterglow nanoparticles with photosensitizer tetrabromorhodamine-123 (TBrRh123), and as a result, it caused the generation of singlet oxygen for PDT cancer treatment. Moreover, these ZnS:Cu,Co nanoparticles show long-lasting afterglow, which constantly acts as a light source for photodynamic therapy (PDT) activation. Efficient energy transfer from ZnS:Cu,Co nanoparticles to TBrRh123 also has been proven because the absorption spectrum of the TBrRh123 photosensitizer overlaps ZnS:Cu,Co luminescence and afterglow spectra. As for *in vitro* studies, it was revealed that a high dose of X-ray irradiation is preferred, but that an X-ray dose of 3 Gy is already enough because it starts to cause apparent hazard effects on the PC3 cell. In addition, upon X-ray irradiation, the cell metabolic activity was 93% with ZnS:Cu,Co alone, 92% with TBrRh123, and 40% with ZnS:Cu,Co-TBrRh123 conjugates. Thus, the preliminary *in vitro* experiments on prostate cancer cells resulted that X-ray-activated ZnS:Cu,Co-TBrRh123 conjugates are very effective for cancer cell destruction.

It was also found that the recently invented copper–cysteamine complex (Cu-Cy) nanoparticles can be activated directly by X-ray to produce singlet oxygen [46]. The RNO-ID method was used for the detection of singlet oxygen irradiated at different X-ray doses. Singlet oxygen production was also measured using ZnO nanoparticles and photosensitizer protoporphyrin IX (PpIX) in the same amount and under the same conditions for comparison with Cu–Cy nanoparticles. It was determined that ZnO nanoparticles had the lowest quantum yield of ROS, and Cu–Cy nanoparticles have the highest one in comparison with all the others. In addition, Cu-Cy particles can produce singlet oxygen upon the activation by UV, and the efficiency is similar to that of PpIX. Due to that, these Cu–Cy nanoparticles may be used as a new type of photosensitizer that can be activated by both light and X-ray, and therefore, it can enable PDT for skin cancer and deep cancer treatment. Furthermore, the cell viability gradually reduced from ~95% to ~70% when the Cu–Cy concentration increased from 0.1 μg/mL to 200 μg/mL. Therefore, these nanoparticles have low toxicity at these concentrations. Recently, the same copper-cysteamine (Cu-Cy) nanoparticles were synthesized and used for XPDT without additional photosensitizer by Shrestha *et al.* [47]. Moreover, these nanoparticles were conjugated to a pH-low insertion peptide (pHLIP) to obtain active targeting to low pH tumors in the future. Cu-Cy nanoparticles were used in therapy for CRL-2116 cell lines. Experiments were conducted on mice irradiated 30 min after injection of particles with an X-ray irradiation dose of 5 Gy (90 kVp, 30 mA). It was shown that pHLIP-conjugated Cu-Cy nanoparticles reduced tumor size in both male and female mice, probably because of pHLIP that bound Cu-Cy directly to a cell and thus contributed to the enhancement effect.

Abliz *et al.* [48] reported on a novel non-invasive methodology of utilizing "soft" energy diagnostic X-rays to indirectly activate a photo-agent for photodynamic therapy (PDT). Some photosensitizer such as photofrin II (Photo II) was activated *via* X-ray induced luminescence from Gadolinium Oxysulfide (20-micron dimension) particles doped with Terbium ($Gd_2O_2S:Tb$). Photodynamic agents, for example, Photo II, that are utilized in PDT processes, have a remarkable property to become preferentially retained within the tumor's micro-environment. Strong suppression (about > 90% relative to controls) in the cellular metabolic activity of human glioblastoma was obtained due to the therapy, which included such steps as the addition of clinically relevant con-

centrations of 20 μg/ml Photo II with Gd_2O_2S:Tb particles and 120 kV diagnostic X-ray irradiation for 15 minutes.

Furthermore, liposomes have been well established as an effective drug delivery system because of its simplicity of synthesis and unique properties. Deng *et al.* [49] reported X-ray-activated liposomes in combination with gold nanoparticles and verteporfin (VP) as a photosensitizer. The singlet oxygen is generated due to the 6 MeV X-rays induced verteporfin, and, as a result, it destroys the liposomal membrane and causes the release of cargos from the liposomal cavity. This release strategy has the capacity for *in vitro* destruction of genes and enhanced efficacy of killing cancer cells. Besides, the toxicity of liposomes doped with gold nanoparticles and VP was analyzed. It was found that no significant change was observed in the viability of PC12 cells treated with liposome (concentrations up to 50 μM).

Chen and co-workers [50] investigated an effective non-invasive approach by using a combination of Tb^{3+}-doped LaF_3 scintillating NPs (LaF_3: Tb) with sizes approximately 25 nm and photosensitizer (meso-tetra (4-carboxyphenyl) porphyrin (MTCP)) followed by activation with soft X-ray irradiation for 1 min (10 mA and 80 kV). The experiment was conducted on a 9L glioma cell line. The results showed that the cell viability was decreased when cells were irradiated with X-ray. Particularly, the viability of 3T3 fibroblast cells significantly reduced from 77% to 28% when LaF_3: Tb-MTCP groups were excited by X-ray. In addition, NPs have good dispersibility in aqueous solution, high biocompatibility and therefore, the cytotoxicity effect was not obviously assumed. A proof of concept as a non-invasive way to treat brain cancer in the future was demonstrated. Another group of researchers, Elmenoufy *et al.* [51], also studied these highly stable in colloid and biocompatible LaF_3:Tb NPs conjugated with Rose Bengal photosensitizer (RB) that could generate a reasonable amount of $^1O_2$. It was determined that the amount of $^1O_2$ induced by ScNPs–RB nanocomposites was much higher than ScNPs or RB alone.

Another good example is conjugates of CeF_3 nanoparticles with the VP photosensitizer that was studied by Clement *et al.* [52]. These CeF_3 nanoparticles were synthesized using a simple co-precipitation route and then conjugated with the photosensitizer *via* mixing in a rotator at room temperature for 6 h. During X-ray exposure (45 kV/40 mA), this composite nanomaterial is able to generate singlet oxygen that was measured using a SOSG fluorescent probe. It happens because of the CeF_3 nanoparticle emission spectrum (peaking at around 340 nm upon irradiation with 8 keV X-ray) that with 30% overlaps with the Soret absorption band of an optical absorption spectrum of VP. Moreover, the viability of pancreatic cancer cells treated with the CeF_3-VP conjugate is reduced so that 32% of the cells were killed at 6 Gy radiation dose.

It was revealed by Kaščáková *et al.* [53] that a liponanoparticle based on $GdEuC_{12}$ micelles incorporating hypericin as a photosensitizer in their hydrophobic core provides X-ray induced singlet oxygen production. It is necessary to point out that this approach can be used for different types of liponanoparticles or other photosensitizers. For example, liposomes that are already widely used in medical applications and can be easily adapted to various biological purposes can also be used in this therapy. The main advantage of using micelles is that its micellar structure can integrate highly hydrophobic molecules such as typical photosensitizers to sites of interest, overcoming their poor water solubility. Upon X-ray irradiation of the Hyp-$GdEuC_{12}$ micelles, the characteristic Eu^{3+} luminescence in the visible region was detected. I It was observed that increasing Hyp concentration in the micelle causes a decrease of Eu^{3+} luminescence. This fact gives evidence of an energy transfer from europium to the hypericin following by X-ray excitation. Analysis of singlet oxygen generation using mass spectrometry with methoxyvinylpyrene (MVP) as a singlet oxygen probe showed that upon X-ray irradiation, singlet oxygen production increases with increasing Hyp concentration in the Hyp-$GdEuC_{12}$ micelles.

Bulin *et al.* [54] presented another biocompatible nanohybrid system, including a terbium oxide nanoscintillator coated with a polysiloxane layer (Tb_2O_3@SiO_2) and a PS (porphyrin), in which energy is transferred. These Tb_2O_3@SiO_2 NPs were prepared by a two-step synthesis. Firstly, Tb_2O_3 was formed in diethylene glycol (DEG), and after that, the polysiloxane shell formation was caused by hydrolysis−condensation of appropriate silane precursors. The diameter of the synthesized core is about 3 nm, while the average size of the core−shell particles is about 10 nm. The production of singlet oxygen under X-ray radiation was pointed out using two commercial probes: the singlet oxygen sensor green (SOSG) and the 3′-p-(aminophenyl) fluorescein (APF). It was determined that an enhancement of the number of formed $^1O_2$ in solution is related to the increase of X-ray dose.

Recently, Zhang *et al.* [55] presented another efficient NPs-PS nanocomposite of β-$NaGdF_4$:Tb^{3+} spherical-like nanoparticles with Rose Bengal PS. It can be a promising platform for *in vivo* XPDT in deep tumors because upon X-ray irradiation spectrum of NPs emission excellent overlaps with RB absorption. It should be noted that the as-prepared $NaGdF_4$:Tb^{3+} NPs are hydrophobic, so they are not suitable for biomedical application. Thus, the NPs surface was modified with an amino group using 2-minoethylphosphonic acid (AEP) to obtain biocompatibility and water-dispersity. NPs-RB conjugate will generate singlet oxygen *via* FRET under X-ray irradiation, particularly the X-ray tube was set to 80 kV and 0.5 mA level. The best XPDT efficacy during *in vivo* experiments was obtained for the experimental group irradiated for 90 min (1.17 Gy) that caused over 80% of cell death. Similar to the above-mentioned nanocomposite was studied by Zhang *et al.* [56]. According to their research, the β-$NaLuF_4$:Tb^{3+} spherical NPs were coupled with RB photosensitizer *via* covalent bonding. The NPs surface was modified with hydrophilic decoration by the ligand-exchanged method to obtain the biocompatibility of such a nanocomposite. It was also shown that the excitation spectrum of β-$NaLuF_4$:15% Tb^{3+} NPs perfectly overlaps with the absorption spectrum of RB at 545 nm upon X-ray excitation. It was also found that the NPs and NPs−RB are water-soluble and noncytotoxic since the viability of HepG2 cells incubated with different concentrations of NPs or NPs−RB was about 95%. These results prove that NPs and NPs−RB are water-

soluble and noncytotoxic. Compared to the above-mentioned research, this synthesized NPs−RB nanocomposite showed significant antitumor efficiency up to 80 ± 12.3% with a total X-ray dose of only 0.19 Gy.

Popovich *et al.* [57] synthesized and characterized Lu-AG:Pr^{3+}@SiO_2-PpIX nanocomposite with an average diameter of about 30 nm, which consists of $Lu_3Al_5O_{12}$:Pr^{3+} core (LuAG:Pr^{3+}), silica (SiO_2) shell and protoporphyrin IX (PpIX) as a photosensitizer. The preparation of this nanomaterial includes three steps: photo-induced precipitation of the LuAG:Pr^{3+} core, sol-gel approach for amorphous silica coating, and a biofunctionalization by attaching the PpIX molecules. It was shown that the absorption spectrum of PpIX and the emission spectrum of LuAG:Pr^{3+} overlap with each other in both the Soret band (around 400 nm) and Q-bands (between 500 and 650 nm). This suggests an energy transfer from Pr^{3+} to the photosensitizer molecules. As a result, the singlet oxygen was generated in the system, and this process was monitored by the APF chemical probe that is sensitive to the singlet oxygen presence.

Another novel nanocomposite material that can be useful in XPDT was synthesized by Procházková *et al.* [58]. It is based on a scintillating ZnO:Ga core that is coated with the SiO_2 shell facilitating a functionalization by a protoporphyrin PpIX layer as a photosensitizer. An overlap between the absorption spectrum of PpIX and RL spectrum of ZnO:Ga proves an efficient energy transfer between the nanoparticle core and the PpIX outer layer in the functionalized sample. Using the APF chemical probe, it was also demonstrated the ability of ZnO:Ga@SiO_2-PpIX nanocomposite to generate singlet oxygen. Furthermore, it was noted that the modification of ZnO:Ga core by doping with Mg or Cd ions would increase the efficiency of energy transfer between the core and photosensitizer and, as a result, also the singlet oxygen generation [59].

A new method based on $LiLuF_4$:Ce@SiO_2@Ag_3PO_4@Pt(IV) nanoparticles (LAPNP) is presented by Wang *et al.* [60]. The synthesis technique consists of $LiLuF_4$:Ce scintillating nanoparticles preparation following by their coating with SiO_2, loading their surface with Ag_3PO_4 semiconductor nanoparticles as the photosensitizer, and finally modifying these structures with a cisplatin prodrug Pt (IV). This cisplatin prodrug is used to increase the yield of hydroxyl radicals (·OH) by increasing the separation of electrons and holes in photosensitizers. The fluorescence spectrum of $LiLuF_4$:Ce and the absorption spectrum of Ag_3PO_4 were characterized, and it was shown that upon X-ray irradiation (80 kV), the fluorescence peaks of $LiLuF_4$:Ce occurred at 305 and 325 nm, and for Ag_3PO_4, the absorption peak occurred at 295 nm. However, the absorption of Ag_3PO_4 and the fluorescence of $LiLuF_4$:Ce were still compatible. Also, the ability of LAPNP to produce ·OH upon irradiation with hard rays (6 MeV) in solution was measured. During the *in vitro* experiments conducted on HeLa cells in the presence of 6 MeV X-ray, it resulted that LAPNP produced ·OH efficiently in cancer cells and caused more DNA damage compared with the same NPs without PS. Besides, the analysis of change in the tumor volumes was carried out. It was found that after irradiation, the growth of the tumors treated with LAPNP and X-ray was suppressed.

Ahmad *et al.* [61] studied the scintillating CeF_3:Gd^{3+},Tb^{3+} nanoparticles for use as a viable clinical tool in the treatment of deep-seated tumors. These theranostic NPs were coated with mesoporous silica and then loaded with Rose Bengal as a photosensitizer (CGTS-RB). The generation of singlet oxygen in tumors located deep within the tissue could be done with a single X-ray dose of 3 Gy. As for toxicity, the CGTS-RB nanoparticles were accumulated mostly in the liver, spleen, and lungs and these collections were gradually cleared within 30 days. Also, no organ damage or inflammation was observed, therefore, it was concluded that CGTS-RB NPs had no short- or long-term *in vivo* toxicities. Moreover, 4T1, Renca, and Mgc803 cell viability after X-ray irradiation of 1 Gy reduced to 90%, 84%, 82%, and 53%, 49.6%, and 50% for the CGTS and CGTS-RB groups, respectively. Thus, it is indicated that XPDT treatment was four times more lethal to cells than radiotherapy treatment alone. Besides, it was revealed that a single dose of 6 Gy or even 3 Gy CGTS-RB had the highest treatment efficacy and using CGTS-RB had a considerably better curative effect than CGTS NPs alone.

It was shown by Wang *et al.* [62] that conjugation of scintillator $SrAl_2O_4$:Eu^{2+} (SAO: Eu) and a photosensitizer MC540 co-loaded mesoporous silica nanoparticles (MC540-SAO:Eu@mSiO_2) can produce singlet oxygen $^1O_2$ under X-ray radiation. It should be noted that all the components, such as MC540, SAO:Eu, and SiO_2, have no toxic effect without irradiation. As for *in vitro* studies, after injection to H1299 cells and the applied radiation (with 50 kV X-ray at 0.83, 1.67, 3.33, and 5 Gy), cell viability was reduced to 31.4 ± 2.3%, 19.6 ± 4.6%, 18.6 ± 7.4%, and 17.5 ± 5.6%, respectively. As for *in vivo* experiments, after X-ray radiation (50 kV) for a dose of 5 Gy, the tumor growth was monitored by bioluminescence imaging (BLI), and it was revealed that the BLI signals were significantly suppressed in X-PDT treated animals. It is necessary to note that the MC540-SAO:Eu@mSiO_2 nanoparticles are decayed after the end of treatment and efficiently cleared from the hosts.

Recently, Chen *et al.* [63] used to treat tumors in internal organs a photosensitizer, 2, 3-naphthalocyanine (NC), and LGO:Cr nanoparticles. This nanocomposite was encapsulated into mesoporous silica nanoparticles and, thus, formed nanoscintillators about 100 nm in size. To obtain effective accumulation into H1299 lung cancer tumors after intravenous therapy, it was necessary to PEGylate and conjugate these nanoparticles with cetuximab. Analysis of the X-ray luminescence from LGO:Cr confirmed the fact that nanoconjugates were able to effectively accumulate in lung tumors. The $^1O_2$ production was analyzed both in a PBS solution with singlet oxygen sensor green (SOSG) and *in vitro* with H1299 cells upon X-ray irradiation (0–4 Gy). In these cases, using NC with X-ray, LGO:Cr@mSiO_2 with X-ray or X-ray alone caused an increase of luminescence slightly. As for the combination of NC, LGO:Cr@mSiO_2, and X-rays, it led to a significant, time-dependent increase of fluorescence intensity that indicates efficient production of $^1O_2$ by these nanoparticles both in solution and in the cells. Notably, there was no detectable cell viability drop when the cells were treated with NC-LGO:Cr@mSiO_2 nanoparticles alone and X-ray alone. On the other hand, the treatment with a combination of NC-

LGO:Cr@mSiO$_2$ and X-ray led to efficient cell death. Particularly, it was determined that the cell viability was reduced to 46.4 ± 7.4% (50 μg/mL of NC-LGO:Cr@mSiO$_2$ and 2 Gy irradiation).

Song *et al.* [64] took into account the fact that according to some research, high-dose X-ray irradiation inevitably has a hazardous effect on normal tissues and, thus, they reported a strategy for cancer treatment by using low-dose X-ray-activated persistent luminescence nanoparticle (PLNP) as an excitation source. They synthesized W(VI)-doped $ZnGa_2O_4$:Cr PLNPs that showed stronger persistent luminescence intensity and longer persistent luminescence time compared to the traditional $ZnGa_2O_4$:Cr PLNPs. It should be noted that even after stopping the X-ray irradiation, the persistent luminescence signal was still detected within 6 hours. After that, PLNPs were conjugated with Zn(II) phthalocyanine tetrasulfonic acid (ZnPcS4) as the photosensitizer. The results of *in vitro* experiment showed that ZGO:Cr/W–ZnPcS4 nanoplatform (after 2 min X-ray irradiation, 0.09 Gy/min) caused a considerable cell-killing effect. Thus, after 2 min excitation, the reduction in viability of HeLa cells to about 40%. Additionally, the increased concentrations of this nanoplatform led to decreased cell viability. As for *in vivo* experiments, this nanocomposite was activated with X-ray irradiation (0.09 Gy/min), and monitoring of fluorescence of the ZGO:Cr/W–ZnPcS4 nanoplatform showed that it is still increased and gradually remained unchanged (more than 40 min) while the persistent luminescence decayed. Also, it was determined that the tumor growth was significantly inhibited within 1 week and effectively suppressed in about 16 days in the experimental group treated with a combination of ZGO:Cr/W–ZnPcS4 nanoplatform and X-ray due to the high-efficiency production of $^1O_2$ from the nanoplatform. Furthermore, pycnosis and karyolysis of cancer cells were observed in this experimental group confirming that the malignant tissues were obviously damaged after XPDT treatment. Thus, Song *et al.* demonstrated that low-dose (2 min, 0.09 Gy/min) X-ray irradiation can be used to activate the ZGO:Cr/W–ZnPcS4 nanoplatform and cause a significant inhibitory effect on tumor progression in both *in vitro* and *in vivo* experiments. In addition, the low toxicity of nanoplatform under research was revealed after confirmation of the absence of obvious damage to the organs after PDT treatment using histological analysis of major organs.

3.3. Metal Nanoparticles

The gold nanotriangles (AuNTs) were introduced as a possible X-ray radiotherapy sensitizer. Thus, Bhattarai *et al.* [65] prepared AuNTs and functionalized them with mPEG-SH of various molecular weights. After analysis of this nanomaterial, they performed *in vivo* biodistribution and tumor growth delay experiments to determine if PEGylated AuNTs (pAuNTs) accumulated in a U87MG tumor or not. Besides, a substantial amount of gold was detected in tumors compared to the muscle, brain, heart, and blood, even within 24 h after injection. In the experiment, cells were treated or internalized with pAuNTs for 24 h and then irradiated with X-ray (250 kV). This approach was significantly more effective at reducing the surviving cell population compared to radiotherapy alone at 4 Gy and 6 Gy. It was also demonstrated that pAuNTs alone do not cause tumor growth inhibition. Moreover, the average volume of tumors in the experimental group (with a combination of radiotherapy and pAuNTs) was significantly smaller than that of mice in the group with applied radiotherapy only. This fact translated to a trend towards improved survival of mice treated with pAuNTs and X-ray. Thus, the survival rate of mice was 0%, 20% and 30% for the experimental groups treated with vehicle alone, radiotherapy alone, and a combination of radiotherapy and pAuNTs, respectively. Thus, pAuNTs could be used as an effective radiosensitizer.

Much earlier, the photosensitizing and radiosensitizing effects of 5-aminolevulinic acid (5ALA)-conjugated gold NPs about 34 nm in size were investigated in a study by Mohammadi and co-workers [66]. Experiments were conducted on the Mel-Rm cell line. It should be noted that gold NPs alone, as well as the conjugate of 5ALA and gold NPs, were found to be toxic on the cell line in the applied concentrations. After incubation of the drugs, the different experimental groups were irradiated independently with X-ray treatments at 2, 4, 6, 8, 10, 12, and 16 Gy radiation doses (X-ray tube with 100 kVp). Also, radiation sensitivity of the cell types of the Mel-Rm cell line was obtained using beams of gamma rays at a dose of 30 Gy and showed significant differences in cell survival for this treatment group compared to the control group. In X-ray treatments, any effective enhancement treatment was obtained in the presence of a conjugate. Particularly, for cells with (5ALA)-conjugated gold NPs, a significant difference between the control group and 4 and 6 Gy dose groups was determined, while groups with another radiation dose showed a slight decrease in cell survival. This can be explained by the fact that the Mel-Rm cell line is radiation-resistant or the X-ray dose for this cell line was insufficient. Moreover, it was determined that cell survival was 30% and 60% in the experimental groups treated with conjugate and gold NPs, respectively.

3.4. Hybrid Nanoparticles

As already mentioned, dense inorganic nanoparticles could be used as promising radiosensitizers because these scintillating nanoparticles can transfer energy to conjugated photosensitizers to enhance the production of ROS and provide UV-visible emission. For example, Bekah *et al.* [67], using a hydrothermal method, synthesized LaF_3 nanoparticles with surface modification with alendronate and followed by doping with cerium, terbium, or both ($La_{0.6}Ce_{0.2}Tb_{0.2}F_3$-PEG). Then, PEG and such photosensitizers as chlorin e6 or Rose Bengal were conjugated to these NPs. To analyze X-ray induced scintillation, NPs within a B16 cell were placed inside an X-ray machine (150 kV and 20 mA), and then it was determined that NPs have good spectral overlap with chlorin e6 or Rose Bengal photosensitizer molecules. Results of using composite nanomaterial for demonstration radiation dose enhancement in B16 melanoma cells were shown to be successful. Additionally, it was determined that the free photosensitizers and the conjugated nanoparticles accumulated preferentially in the cytoplasm. Moreover, the results of cytotoxicity that was conducted on B16 cells revealed that the nanoparticles exhibited less than 10% toxicity up to a concentration of approximately 5 mg/mL (42 μM).

Zou *et al.* [68] studied the use of $LaF_3:Ce^{3+}$ luminescent nanoparticles as an intracellular light source for photodynamic activation in prostate cancer cells. These nanoparticles were synthesized with a wet-chemistry method in dimethyl sulfoxide (DMSO). The spectroscopic data showed successful encapsulation into the PLGA microspheres of $LaF_3:Ce^{3+}$/DMSO nanoparticles and $LaF_3:Ce^{3+}$/DMSO/PpIX nanoparticles. Compared with the $LaF_3:Ce^{3+}$/DMSO nanoparticles, the fluorescence intensity of the $LaF_3:Ce^{3+}$ is decreased in the $LaF_3:Ce^{3+}$/DMSO/PpIX conjugates. Thus, it was found that under X-ray irradiation, the $LaF_3:Ce^{3+}$/DMSO/PpIX/PLGA conjugate induced cell killing, while the microspheres without PpIX did not enhance the radiation effects; for example, $LaF_3:Ce^{3+}$/DMSO/PpIX/PLGA decreased the viability of PC3 cells almost to 60%. X-ray irradiation (90 kV and 5 mA) was performed at a dose rate of 0.5 Gy/min. As for toxicity, the results showed that the nanoparticles and the particle–PPIX nanocomposites are acceptable for applications. However, it was revealed that the $LaF_3:Ce^{3+}$/PPIX-containing microspheres were found to be 20% more toxic to the cells compared to the $LaF_3:Ce^{3+}$-containing microspheres.

It was mentioned previously that lanthanide-doped fluoride (*e.g.*, $LaF_3:Ce^{3+}$, $LaF_3:Tb^{3+}$) or CeF_3 nanoparticles have been used as radioluminescent sources for common photosensitizers such as porphyrins or Rose Bengal. A new type of sensitizer has recently been studied by Kirakci *et al.* [69]. The octahedral molybdenum cluster compound $(n\text{-}Bu_4N)_2[Mo_6I_8(OOC\text{-}1\text{-}adamantane)_6]$ is suggested to be an efficient sensitizer of singlet oxygen upon X-ray excitation. Its high proton number that increases the interaction probability with X-ray and relevant photophysical properties (in the solid-state or the form of NPs) is the advantage over porphyrins. It was noted a concept that makes energy transfer from the nanoscintillator to the photosensitizer unnecessary because this compound can act as a nanoscintillator and sensitizer of singlet oxygen at the same time. It can help to delete energy losses occurring during energy transfer. Recently, Kirakci *et al.* [70] also prepared other nanoparticles made of the octahedral molybdenum cluster compound $(n\text{-}Bu_4N)_2[Mo_6I_8(OCOCF_3)_6]$ and demonstrated that under X-ray irradiation by a soft X-ray source with a peak energy of 100 keV, this nanocomposite can directly produce singlet oxygen molecules. The results of *in vitro* experiment showed that after incubation of HeLa cells with nanoparticles (8 μg/mL) for 2 hours, a decrease in cell viability of 32% was observed at 1 Gy and 2 Gy, and 59% at 4 Gy compared to irradiated cells in the absence of nanoparticles.

The new theranostic scintillator nanoparticle composite $NaLuF_4$:Gd(35%),Eu(15%)@$NaLuF_4$:Gd(40%)@$NaLuF_4$:Gd (35%),Tb(15%) in a core−shell−shell arrangement was studied by Hsu *et al.* [71]. After all the modifications, ScNP-PAH-RBPEG-FA was prepared for research. The main property of this nanomaterial is the ability to emit several wavelengths upon X-ray radiation. The ScNPs can emit visible light at 543 nm (from Tb^{3+}) to cause the death of cancer cells (MDA-MB-231 and MCF-7) by stimulating the Rose Bengal photosensitizer, and this composite can also emit light at 614 and 695 nm (from Eu^{3+}) for luminescence imaging. Thus, a nanocomposite of these scintillator nanoparticles and appropriate photosensitizers such as RB and biomarker derivatives can generate $^1O_2$ molecules and can be applied for targeted PDT of deep tumor tissue. In addition, results of the analysis of $^1O_2$ generation by the ScNP-PAH-RBPEG-FA and ScNP-$mSiO_2$-PAH-RB-PEG-FA without and with the $mSiO_2$ layer under X-ray excitation showed that a significantly higher percentage of $^1O_2$ was produced for the ScNP-PAH-RB-PEG-FA without the $mSiO_2$ layer (up to 10 Gy X-ray dose). *In vitro* experiments showed that 31% MDA-MB-231 and 21% MCF-7 cancer cells were killed at a radiation dose of 5 Gy.

Liu *et al.* [72] reported another hybrid NPs. The ROS-responsive polymers, poly (thiodiethylene adipate) (PSDEA) and PEG−PSDEA−PEG, were synthesized, and they formed the polymeric NPs, which were encapsulated a nonpolar camptothecin analog, a free drug SN38, for treating malignant tumors with X-ray irradiation. The results clearly demonstrate the effective response of the SS-NPs (the SN38-loaded ROS-responsive NPs) in mediating drug release to the X-ray irradiation at the doses of both 10 and 15 Gy (the cell viability reduced to 30% and 20%, respectively). Thus, the use of combined SS-NPs and X-ray treatment showed essentially full inhibition of tumor growth similar to the free SN38 and X-ray approach, indicating the effective drug release upon the activation of SS-NPs by X-ray irradiation.

Recently, Clement *et al.* [73] showed that an X-ray-induced PDT system where poly (lactide-co-glycolide) (PLGA) polymeric nanoparticles (NPs) incorporating verteporfin (VP) as a photosensitizer can be used to generate cytotoxic singlet oxygen. To enhance cellular uptake, the surface of PLGA-VP NPs was successfully conjugated with folic acid (FA). In this research, a combination of normal (CCD 841 CoN) and cancer cells (HCT116) was used to test cell viability after treatment with conjugates and various doses of 6 MeV X-ray. It was determined that normal cells were not visibly affected by X-ray radiation, while the viability of cancer cells was reduced with different doses; for example, it decreased by 78% at 4 Gy radiation. Clement *et al.* showed that X-ray irradiation (4 Gy) alone can kill 22% of the cancer cells, whereas a combination of radiation with FA-PLGA-VP constructs in these cells can kill about 67%. Thus, according to *in vitro* experiments, this FA-PLGA-VP nanocomposite effectively reduces HCT116 cells in the presence of 6 MeV X-ray radiation.

CONCLUSION

PDT is a promising method of cancer treatment, but nevertheless, it has such limitations to the application as penetration depth. To overcome this limitation, X-ray can be used because it can easily penetrate human tissue. Thus, the use of X-ray to excite PDT has been a promising prospect for longer than 10 years.

After the analysis of all articles from the references, it can be noted that a lot of prospective studies have been carried out on the rare-earth-element based NPs-PS nanocomposite because rare-earth-element-based scintillating NPs have tunable emission wavelengths. Moreover, hybrid and metal NPs have also been studied as a basis for XPDT. All studied NPs were in size from 10 nm to 200 nm, thus they could penetrate cell membranes. In addition, to obtain a good

biodistribution and promising cell uptake, NPs were coated with such biocompatible materials as PLGA and PEG.

A lot of research has been done over the past 10 years, and it was determined that several NPs-PS nanocomposites may exhibit anticancer activity in *in vitro* and *in vivo* experiments. However, XPDT methods still need to be improved to obtain lox toxicity, accurate tumor targeting, and higher therapeutic effects for tumor tissues located more deeply within the body using lower doses of radiation. Thus, although NPs are still in the initial stages of clinical trials, it is hoped that further studies in this field will contribute to successful clinical trial translations.

LIST OF ABBREVIATIONS

PDT	=	Photodynamic Therapy
XPDT	=	X-ray Photodynamic Therapy
PS	=	Photosensitizer
ROS	=	Reactive Oxygen Species
NPs	=	Nanoparticles
ScNPs	=	Scintillating Nanoparticles
QDs	=	Quantum Dots
PpIX	=	protoporphyrin IX
RB	=	Rose Bengal
VP	=	Verteporfin

CONSENT FOR PUBLICATION

Declared None.

CONFLICT OF INTEREST

Declared None.

FUNDING

The authors acknowledge Russian Science Foundation grant # 19-15-00305 for financial support.

ACKNOWLEDGEMENTS

D.Yu. Kirsanova, as the corresponding author, has made a great contribution to the conception and drafting of the work, analysis, and systematization of information. Z.M. Gadzhimagomedova helped with the analysis and systematization of data for this work. A.V. Solatov made the acquisition of information for the manuscript. Both A.Yu. Maksimov, as a medical professional, and A.V. Soldatov carried out proofreading and revising of work for intellectual content. All authors have read and approved the final manuscript.

REFERENCES

[1] World Health Organization Statistical Information System. WHO mortality database. http://www.who.int/healthinfo/statistics/mortality_rawdata/en/index.html

[2] Malvezzi, M.; Carioli, G.; Bertuccio, P.; Boffetta, P.; Levi, F.; La Vecchia, C.; Negri, E. European cancer mortality predictions for the year 2019 with focus on breast cancer. *Ann. Oncol.,* **2019**, *30*(5), 781-787. http://dx.doi.org/10.1093/annonc/mdz051 PMID: 30887043

[3] Abrahamse, H.; Kruger, C.A.; Kadanyo, S.; Mishra, A. Nanoparticles for Advanced Photodynamic Therapy of Cancer. *Photomed. Laser Surg.,* **2017**, *35*(11), 581-588. http://dx.doi.org/10.1089/pho.2017.4308 PMID: 28937916

[4] Robertson, C.A.; Evans, D.H.; Abrahamse, H. Photodynamic therapy (PDT): a short review on cellular mechanisms and cancer research applications for PDT. *J. Photochem. Photobiol. B,* **2009**, *96*(1), 1-8. http://dx.doi.org/10.1016/j.jphotobiol.2009.04.001 PMID: 19406659

[5] Kamkaew, A.; Chen, F.; Zhan, Y.; Majewski, R.L.; Cai, W. Scintillating Nanoparticles as Energy Mediators for Enhanced Photodynamic Therapy. *ACS Nano,* **2016**, *10*(4), 3918-3935. http://dx.doi.org/10.1021/acsnano.6b01401 PMID: 27043181

[6] Larue, L.; Ben Mihoub, A.; Youssef, Z.; Colombeau, L.; Acherar, S.; André, J.C.; Arnoux, P.; Baros, F.; Vermandel, M.; Frochot, C. Using X-rays in photodynamic therapy: an overview. *Photochem. Photobiol. Sci.,* **2018**, *17*(11), 1612-1650. http://dx.doi.org/10.1039/C8PP00112J PMID: 29938265

[7] Ren, X.D.; Hao, X.Y.; Li, H.C.; Ke, M.R.; Zheng, B.Y.; Huang, J.D. Progress in the development of nanosensitizers for X-ray-induced photodynamic therapy. *Drug Discov. Today,* **2018**, *23*(10), 1791-1800. http://dx.doi.org/10.1016/j.drudis.2018.05.029 PMID: 29803933

[8] Fan, W.; Huang, P.; Chen, X. Overcoming the Achilles' heel of photodynamic therapy. *Chem. Soc. Rev.,* **2016**, *45*(23), 6488-6519. http://dx.doi.org/10.1039/C6CS00616G PMID: 27722560

[9] Huang, H.-C.; Hasan, T. The "Nano" World in Photodynamic Therapy. *Nanomed Nanotechnol. ,* **2014**, *2*(3)

[10] Lim, C.K.; Heo, J.; Shin, S.; Jeong, K.; Seo, Y.H.; Jang, W.D.; Park, C.R.; Park, S.Y.; Kim, S.; Kwon, I.C. Nanophotosensitizers toward advanced photodynamic therapy of Cancer. *Cancer Lett.,* **2013**, *334*(2), 176-187. http://dx.doi.org/10.1016/j.canlet.2012.09.012 PMID: 23017942

[11] Rancoule, C.; Magné, N.; Vallard, A.; Guy, J.B.; Rodriguez-Lafrasse, C.; Deutsch, E.; Chargari, C. Nanoparticles in radiation oncology: From bench-side to bedside. *Cancer Lett.,* **2016**, *375*(2), 256-262. http://dx.doi.org/10.1016/j.canlet.2016.03.011 PMID: 26987625

[12] Retif, P.; Pinel, S.; Toussaint, M.; Frochot, C.; Chouikrat, R.; Bastogne, T.; Barberi-Heyob, M. Nanoparticles for Radiation Therapy Enhancement: the Key Parameters. *Theranostics,* **2015**, *5*(9), 1030-1044. http://dx.doi.org/10.7150/thno.11642 PMID: 26155318

[13] Sivasubramanian, M.; Chuang, Y.C.; Chen, N.T.; Lo, L.W. Seeing Better and Going Deeper in Cancer Nanotheranostics. *Int. J. Mol. Sci.,* **2019**, *20*(14)E3490 http://dx.doi.org/10.3390/ijms20143490 PMID: 31315232

[14] Yurt, F.; Tunçel, A. Combined Photodynamic and Radiotherapy Synergistic Effect in Cancer Treatment. *Novel Approaches in Cancer Study,* **2018**, *1*(2), 27-29. http://dx.doi.org/10.31031/NACS.2018.01.000506

[15] Hu, X.; Huang, Y.Y.; Wang, Y.; Wang, X.; Hamblin, M.R. Antimicrobial Photodynamic Therapy to Control Clinically Relevant Biofilm Infections. *Front. Microbiol.,* **2018**, *9*, 1299. http://dx.doi.org/10.3389/fmicb.2018.01299 PMID: 29997579

[16] Yang, Y.; Karakhanova, S.; Werner, J.; Bazhin, A.V. Reactive oxygen species in cancer biology and anticancer therapy. *Curr. Med. Chem.,* **2013**, *20*(30), 3677-3692. http://dx.doi.org/10.2174/09298673113209999165 PMID: 23862622

[17] Bakhmetyev, V.V.; Minakova, T.S.; Mjakin, S.V.; Lebedev, L.A.; Vlasenko, A.B.; Nikandrova, A.A.; Ekimova, I.A.; Eremina, N.S.; Sychov, M.M.; Ringuede, A. Synthesis and surface characterization of nanosized Y2O3:Eu and YAG:Eu luminescent phosphors which are useful in photodynamic therapy of cancer. *Eur. J. Nanomed.,* **2016**, *8*(4) http://dx.doi.org/10.1515/ejnm-2016-0020

[18] Cheng, J.; Tan, G.; Li, W.; Li, J.; Wang, Z.; Jin, Y. Preparation, characterization and *in vitro* photodynamic therapy of a pyropheophorbide-a-conjugated Fe3O4 multifunctional magnetofluorescence photosensitizer. *RSC Advances,* **2016**, *6*(44), 37610-37620. http://dx.doi.org/10.1039/C6RA03128E

[19] Darafsheh, A.; Najmr, S.; Paik, T.; Tenuto, M.E.; Murray, C.B.; Finlay, J.C.; Friedberg, J.S. Characterization of rare-earth-doped nanophosphors for photodynamic therapy excited by clinical ionizing radiation beams.*In Optical Methods for Tumor Treatment and Detection: Mechanisms and Techniques in Photodynamic Therapy XXIV*,; , **2015**.

[20] Eshghi, H.; Sazgarnia, A.; Rahimizadeh, M.; Attaran, N.; Bakavoli, M.; Soudmand, S. Protoporphyrin IX-gold nanoparticle conjugates as an efficient photosensitizer in cervical cancer therapy. *Photodiagn. Photodyn. Ther.,* **2013**, *10*(3), 304-312. http://dx.doi.org/10.1016/j.pdpdt.2013.02.003 PMID: 23993857

[21] Hwang, J.W.; Jung, S.J.; Cheong, T.C.; Kim, Y.; Shin, E.P.; Heo, I.; Kim, G.; Cho, N.H.; Wang, K.K.; Kim, Y.R. Smart Hybrid Nanocomposite for Photodynamic Inactivation of Cancer Cells with Selectivity. *J. Phys. Chem. B,* **2019**, *123*(31), 6776-6783. http://dx.doi.org/10.1021/acs.jpcb.9b04301 PMID: 31310131

[22] Idris, N.M.; Gnanasammandhan, M.K.; Zhang, J.; Ho, P.C.; Mahendran, R.; Zhang, Y. *In vivo* photodynamic therapy using upconversion nanoparticles as remote-controlled nanotransducers. *Nat. Med.,* **2012**, *18*(10), 1580-1585. http://dx.doi.org/10.1038/nm.2933 PMID: 22983397

[23] Iqbal, S.; Fakhar-E-Alam, M.; Atif, M.; Ahmed, N.; -Ul-Ahmad, A.; Amin, N.; Alghamdi, R.A.; Hanif, A.; Farooq, W.A. Empirical Modeling of Zn/ZnO Nanoparticles Decorated/Conjugated with Fotolon (Chlorine e6) Based Photodynamic Therapy towards Liver Cancer Treatment. *Micromachines (Basel),* **2019**, *10*(1)E60 http://dx.doi.org/10.3390/mi10010060 PMID: 30658388

[24] Shimoyama, A.; Watase, H.; Liu, Y.; Ogura, S.; Hagiya, Y.; Takahashi, K.; Inoue, K.; Tanaka, T.; Murayama, Y.; Otsuji, E.; Ohkubo, A.; Yuasa, H. Access to a novel near-infrared photodynamic therapy through the combined use of 5-aminolevulinic acid and lanthanide nanoparticles. *Photodiagn. Photodyn. Ther.,* **2013**, *10*(4), 607-614. http://dx.doi.org/10.1016/j.pdpdt.2013.07.005 PMID: 24284118

[25] Wang, S.; Wang, H.; Song, C.; Li, Z.; Wang, Z.; Xu, H.; Yu, W.; Peng, C.; Li, M.; Chen, Z. Synthesis of Bi_2WO_{6-x} nanodots with oxygen vacancies as an all-in-one nanoagent for simultaneous CT/IR imaging and photothermal/photodynamic therapy of tumors. *Nanoscale,* **2019**, *11*(32), 15326-15338. http://dx.doi.org/10.1039/C9NR05236D PMID: 31386732

[26] Wang, W.; Wang, L.; Li, Z.; Xie, Z. BODIPY-containing nanoscale metal-organic frameworks for photodynamic therapy. *Chem. Commun. (Camb.),* **2016**, *52*(31), 5402-5405. http://dx.doi.org/10.1039/C6CC01048B PMID: 27009757

[27] Chen, P.; Huang, Y-F.; Xu, G-Y.; Xue, J-P.; Chen, J-J. Functionalized Eu(III)-based nanoscale metal-organic framework for enhanced targeted anticancer therapy. *J. Porphyr. Phthalocyanines,* **2019**, *23*(06), 619-627. http://dx.doi.org/10.1142/S1088424619500299

[28] Gao, S.; Zheng, P.; Li, Z.; Feng, X.; Yan, W.; Chen, S.; Guo, W.; Liu, D.; Yang, X.; Wang, S.; Liang, X.J.; Zhang, J. Biomimetic O_2-Evolving metal-organic framework nanoplatform for highly efficient photodynamic therapy against hypoxic tumor. *Biomaterials,* **2018**, *178*, 83-94. http://dx.doi.org/10.1016/j.biomaterials.2018.06.007 PMID: 29913389

[29] Liu, J.; Yang, Y.; Zhu, W.; Yi, X.; Dong, Z.; Xu, X.; Chen, M.; Yang, K.; Lu, G.; Jiang, L.; Liu, Z. Nanoscale metal-organic frameworks for combined photodynamic & radiation therapy in cancer treatment. *Biomaterials,* **2016**, *97*, 1-9. http://dx.doi.org/10.1016/j.biomaterials.2016.04.034 PMID: 27155362

[30] Song, M-R.; Li, D-Y.; Nian, F-Y.; Xue, J-P.; Chen, J-J. Zeolitic imidazolate metal organic framework-8 as an efficient pH-controlled delivery vehicle for zinc phthalocyanine in photodynamic therapy. *J. Mater. Sci.,* **2017**, *53*(4), 2351-2361. http://dx.doi.org/10.1007/s10853-017-1716-z

[31] Mokoena, P.P.; Swart, H.C.; Ntwaeaborwa, O.M. Upconversion luminescence of Er3+/Yb3+ doped Sr5(PO4)3OH phosphor powders. *Physica B,* **2018**, *535*, 57-62. http://dx.doi.org/10.1016/j.physb.2017.06.040

[32] Tavakkoli, F.; Zahedifar, M.; Sadeghi, E. Effect of LaF_3: Ag fluorescent nanoparticles on photodynamic efficiency and cytotoxicity of Protoporphyrin IX photosensitizer. *Photodiagn. Photodyn. Ther.,* **2018**, *21*, 306-311. http://dx.doi.org/10.1016/j.pdpdt.2018.01.009 PMID: 29331661

[33] Sengar, P.; Garcia-Tapia, K.; Chauhan, K.; Jain, A.; Juarez-Moreno, K.; Borbón-Nuñez, H.A.; Tiznado, H.; Contreras, O.E.; Hirata, G.A. Dual-photosensitizer coupled nanoscintillator capable of producing type I and type II ROS for next generation photodynamic therapy. *J. Colloid Interface Sci.,* **2019**, *536*, 586-597. http://dx.doi.org/10.1016/j.jcis.2018.10.090 PMID: 30390584

[34] Charron, G.; Stuchinskaya, T.; Edwards, D.R.; Russell, D.A.; Nann, T. Insights into the Mechanism of Quantum Dot-Sensitized Singlet Oxygen Production for Photodynamic Therapy. *J. Phys. Chem. C,* **2012**, *116*(16), 9334-9342. http://dx.doi.org/10.1021/jp301103f

[35] Ge, J.; Lan, M.; Zhou, B.; Liu, W.; Guo, L.; Wang, H.; Jia, Q.; Niu, G.; Huang, X.; Zhou, H.; Meng, X.; Wang, P.; Lee, C.S.; Zhang, W.; Han, X. A graphene quantum dot photodynamic therapy agent with high singlet oxygen generation. *Nat. Commun.,* **2014**, *5*, 4596. http://dx.doi.org/10.1038/ncomms5596 PMID: 25105845

[36] Homayoni, H.; Jiang, K.; Zou, X.; Hossu, M.; Rashidi, L.H.; Chen, W. Enhancement of protoporphyrin IX performance in aqueous solutions for photodynamic therapy. *Photodiagn. Photodyn. Ther.,* **2015**, *12*(2), 258-266. http://dx.doi.org/10.1016/j.pdpdt.2015.01.003 PMID: 25636780

[37] Chen, W.; Zhang, J. Using nanoparticles to enable simultaneous radiation and photodynamic therapies for cancer treatment. *J. Nanosci. Nanotechnol.,* **2006**, *6*(4), 1159-1166. http://dx.doi.org/10.1166/jnn.2006.327 PMID: 16736782

[38] Ostrowski, A.; Nordmeyer, D.; Boreham, A.; Holzhausen, C.; Mundhenk, L.; Graf, C.; Meinke, M.C.; Vogt, A.; Hadam, S.; Lademann, J.; Rühl, E.; Alexiev, U.; Gruber, A.D. Overview about the localization of nanoparticles in tissue and cellular context by different imaging techniques. *Beilstein J. Nanotechnol.,* **2015**, *6*, 263-280. http://dx.doi.org/10.3762/bjnano.6.25 PMID: 25671170

[39] Kaszewski, J.; Olszewski, J.; Rosowska, J.; Witkowski, B.; Wachnicki, Ł.; Wenelska, K.; Mijowska, E.; Gajewski, Z.; Godlewski, M.; Godlewski, M.M. HfO2:Eu nanoparticles excited by X-rays and UV-visible radiation used in biological imaging. *J. Rare Earths,* **2019**, *37*(11), 1176-1182. http://dx.doi.org/10.1016/j.jre.2019.04.003

[40] Sapre, A.A.; Novitskaya, E.; Vakharia, V.; Cota, A.; Wrasidlo, W.; Hanrahan, S.M.; Derenzo, S.; Makale, M.T.; Graeve, O.A.; Optimized Scintillator, Y.A.G. Optimized Scintillator YAG:Pr Nanoparticles for X-ray Inducible Photodynamic Therapy. *Mater. Lett.,* **2018**, *228*, 49-52. http://dx.doi.org/10.1016/j.matlet.2018.05.090 PMID: 30505045

[41] Li, X.; Xue, Z.; Jiang, M.; Li, Y.; Zeng, S.; Liu, H. Soft X-ray activated $NaYF_4$:Gd/Tb scintillating nanorods for *in vivo* dual-modal X-ray/X-ray-induced optical bioimaging. *Nanoscale,* **2017**, *10*(1), 342-350. http://dx.doi.org/10.1039/C7NR02926H PMID: 29215103

[42] Sadjadpour, S.; Safarian, S.; Zargar, S.J.; Sheibani, N. Antiproliferative effects of ZnO, ZnO-MTCP, and ZnO-CuMTCP nanoparticles with safe intensity UV and X-ray irradiation. *Biotechnol. Appl. Biochem.,* **2016**, *63*(1), 113-124. http://dx.doi.org/10.1002/bab.1344 PMID: 25581219

[43] Generalov, R.; Kuan, W.B.; Chen, W.; Kristensen, S.; Juzenas, P. Radiosensitizing effect of zinc oxide and silica nanocomposites on cancer cells. *Colloids Surf. B Biointerfaces,* **2015**, *129*, 79-86. http://dx.doi.org/10.1016/j.colsurfb.2015.03.026 PMID: 25829130

[44] Popovich, K.; Procházková, L.; Pelikánová, I.T.; Vlk, M.; Palkovský, M.; Jarý, V.; Nikl, M.; Múčka, V.; Mihóková, E.; Čuba, V. Preliminary study on singlet oxygen production using CeF3:Tb3+@SiO2-PpIX. *Radiat. Meas.,* **2016**, *90*, 325-328. http://dx.doi.org/10.1016/j.radmeas.2016.01.033

[45] Ma, L.; Zou, X.; Bui, B.; Chen, W.; Song, K.H.; Solberg, T. X-ray excited ZnS:Cu,Co afterglow nanoparticles for photodynamic activation. *Appl. Phys. Lett.,* **2014**, *105*(1) http://dx.doi.org/10.1063/1.4890105

[46] Ma, L.; Zou, X.; Chen, W. A new X-ray activated nanoparticle photosensitizer for cancer treatment. *J. Biomed. Nanotechnol.,* **2014**, *10*(8), 1501-1508. http://dx.doi.org/10.1166/jbn.2014.1954 PMID: 25016650

[47] Shrestha, S.; Wu, J.; Sah, B.; Vanasse, A.; Cooper, L.N.; Ma, L.; Li, G.; Zheng, H.; Chen, W.; Antosh, M.P. X-ray induced photody-

namic therapy with copper-cysteamine nanoparticles in mice tumors. *Proc. Natl. Acad. Sci. USA,* **2019**, *116*(34), 16823-16828. http://dx.doi.org/10.1073/pnas.1900502116 PMID: 31371494

[48] Abliz, E.; Collins, J.E.; Bell, H.; Tata, D.B. Novel applications of diagnostic X-rays in activating a clinical photodynamic drug: Photofrin II through X-ray induced visible luminescence from "rare-earth" formulated particles. *J. XRay Sci. Technol.,* **2011**, *19*(4), 521-530. http://dx.doi.org/10.3233/XST-2011-0311 PMID: 25214384

[49] Deng, W.; Chen, W.; Clement, S.; Guller, A.; Zhao, Z.; Engel, A.; Goldys, E.M. Controlled gene and drug release from a liposomal delivery platform triggered by X-ray radiation. *Nat. Commun.,* **2018**, *9*(1), 2713. http://dx.doi.org/10.1038/s41467-018-05118-3 PMID: 30006596

[50] Chen, M.H.; Jenh, Y.J.; Wu, S.K.; Chen, Y.S.; Hanagata, N.; Lin, F.H. Non-invasive Photodynamic Therapy in Brain Cancer by Use of Tb^{3+}-Doped LaF_3 Nanoparticles in Combination with Photosensitizer Through X-ray Irradiation: A Proof-of-Concept Study. *Nanoscale Res. Lett.,* **2017**, *12*(1), 62. http://dx.doi.org/10.1186/s11671-017-1840-3 PMID: 28110445

[51] Elmenoufy, A.H.; Tang, Y.; Hu, J.; Xu, H.; Yang, X. A novel deep photodynamic therapy modality combined with CT imaging established via X-ray stimulated silica-modified lanthanide scintillating nanoparticles. *Chem. Commun. (Camb.),* **2015**, *51*(61), 12247-12250. http://dx.doi.org/10.1039/C5CC04135J PMID: 26136105

[52] Clement, S.; Deng, W.; Camilleri, E.; Wilson, B.C.; Goldys, E.M. X-ray induced singlet oxygen generation by nanoparticle-photosensitizer conjugates for photodynamic therapy: determination of singlet oxygen quantum yield. *Sci. Rep.,* **2016**, *6*, 19954. http://dx.doi.org/10.1038/srep19954 PMID: 26818819

[53] Kaščáková, S.; Giuliani, A.; Lacerda, S.; Pallier, A.; Mercère, P.; Tóth, É.; Réfrégiers, M. X-ray-induced radiophotodynamic therapy (RPDT) using lanthanide micelles: Beyond depth limitations. *Nano Res.,* **2015**, *8*(7), 2373-2379. http://dx.doi.org/10.1007/s12274-015-0747-5

[54] Bulin, A-L.; Truillet, C.; Chouikrat, R.; Lux, F.; Frochot, C.; Amans, D.; Ledoux, G.; Tillement, O.; Perriat, P.; Barberi-Heyob, M.; Dujardin, C. X-ray-Induced Singlet Oxygen Activation with Nanoscintillator-Coupled Porphyrins. *J. Phys. Chem. C,* **2013**, *117*(41), 21583-21589. http://dx.doi.org/10.1021/jp4077189

[55] Zhang, W.; Zhang, X.; Shen, Y.; Shi, F.; Song, C.; Liu, T.; Gao, P.; Lan, B.; Liu, M.; Wang, S.; Fan, L.; Lu, H. Ultra-high FRET efficiency $NaGdF_4$: Tb^{3+}-Rose Bengal biocompatible nanocomposite for X-ray excited photodynamic therapy application. *Biomaterials,* **2018**, *184*, 31-40. http://dx.doi.org/10.1016/j.biomaterials.2018.09.001 PMID: 30195803

[56] Zhang, X.; Lan, B.; Wang, S.; Gao, P.; Liu, T.; Rong, J.; Xiao, F.; Wei, L.; Lu, H.; Pang, C.; Fan, L.; Zhang, W.; Lu, H. Low-Dose X-ray Excited Photodynamic Therapy Based on $NaLuF_4$:Tb^{3+}-Rose Bengal Nanocomposite. *Bioconjug. Chem.,* **2019**, *30*(8), 2191-2200. http://dx.doi.org/10.1021/acs.bioconjchem.9b00429 PMID: 31344330

[57] Popovich, K.; Tomanová, K.; Čuba, V.; Procházková, L.; Pelikánová, I.T.; Jakubec, I.; Mihóková, E.; Nikl, M. LuAG:Pr^{3+}-porphyrin based nanohybrid system for singlet oxygen production: Toward the next generation of PDTX drugs. *J. Photochem. Photobiol. B,* **2018**, *179*, 149-155. http://dx.doi.org/10.1016/j.jphotobiol.2018.01.015 PMID: 29413988

[58] Procházková, L.; Pelikánová, I.T.; Mihóková, E.; Dědic, R.; Čuba, V. Novel scintillating nanocomposite for X-ray induced photodynamic therapy. *Radiat. Meas.,* **2019**, *121*, 13-17. http://dx.doi.org/10.1016/j.radmeas.2018.12.008

[59] Procházková, L.; Čuba, V.; Beitlerová, A.; Jarý, V.; Omelkov, S.; Nikl, M. Ultrafast Zn(Cd,Mg)O:Ga nanoscintillators with luminescence tunable by band gap modulation. *Opt. Express,* **2018**, *26*(22), 29482-29494. http://dx.doi.org/10.1364/OE.26.029482 PMID: 30470111

[60] Wang, H.; Lv, B.; Tang, Z.; Zhang, M.; Ge, W.; Liu, Y.; He, X.; Zhao, K.; Zheng, X.; He, M.; Bu, W. Scintillator-Based Nanohybrids with Sacrificial Electron Prodrug for Enhanced X-ray-Induced Photodynamic Therapy. *Nano Lett.,* **2018**, *18*(9), 5768-5774. http://dx.doi.org/10.1021/acs.nanolett.8b02409 PMID: 30052464

[61] Ahmad, F.; Wang, X.; Jiang, Z.; Yu, X.; Liu, X.; Mao, R.; Chen, X.; Li, W. Codoping Enhanced Radioluminescence of Nanoscintillators for X-ray-Activated Synergistic Cancer Therapy and Prognosis Using Metabolomics. *ACS Nano,* **2019**, *13*(9), 10419-10433. http://dx.doi.org/10.1021/acsnano.9b04213 PMID: 31430127

[62] Wang, G.D.; Nguyen, H.T.; Chen, H.; Cox, P.B.; Wang, L.; Nagata, K.; Hao, Z.; Wang, A.; Li, Z.; Xie, J. X-Ray Induced Photodynamic Therapy: A Combination of Radiotherapy and Photodynamic Therapy. *Theranostics,* **2016**, *6*(13), 2295-2305. http://dx.doi.org/10.7150/thno.16141 PMID: 27877235

[63] Chen, H.; Sun, X.; Wang, G.D.; Nagata, K.; Hao, Z.; Wang, A.; Li, Z.; Xie, J.; Shen, B. $LiGa_5O_8$:Cr-based theranostic nanoparticles for imaging-guided X-ray induced photodynamic therapy of deep-seated tumors. *Mater. Horiz.,* **2017**, *4*(6), 1092-1101. http://dx.doi.org/10.1039/C7MH00442G PMID: 31528350

[64] Song, L.; Li, P-P.; Yang, W.; Lin, X-H.; Liang, H.; Chen, X-F.; Liu, G.; Li, J.; Yang, H-H. Low-Dose X-ray Activation of W(VI)-Doped Persistent Luminescence Nanoparticles for Deep-Tissue Photodynamic Therapy. *Adv. Funct. Mater.,* **2018**, *28*(18) http://dx.doi.org/10.1002/adfm.201707496

[65] Bhattarai, S.R.; Derry, P.J.; Aziz, K.; Singh, P.K.; Khoo, A.M.; Chadha, A.S.; Liopo, A.; Zubarev, E.R.; Krishnan, S. Gold nanotriangles: scale up and X-ray radiosensitization effects in mice. *Nanoscale,* **2017**, *9*(16), 5085-5093. http://dx.doi.org/10.1039/C6NR08172J PMID: 28134383

[66] Mohammadi, Z.; Sazgarnia, A.; Rajabi, O.; Seilanian Toosi, M. Comparative study of X-ray treatment and photodynamic therapy by using 5-aminolevulinic acid conjugated gold nanoparticles in a melanoma cell line. *Artif. Cells Nanomed. Biotechnol.,* **2017**, *45*(3), 467-473. http://dx.doi.org/10.3109/21691401.2016.1167697 PMID: 27052440

[67] Bekah, D.; Cooper, D.; Kudinov, K.; Hill, C.; Seuntjens, J.; Bradforth, S.; Nadeau, J. Synthesis and characterization of biologically stable, doped LaF3 nanoparticles co-conjugated to PEG and photosensitizers. *J. Photochem. Photobiol. Chem.,* **2016**, *329*, 26-34. http://dx.doi.org/10.1016/j.jphotochem.2016.06.008

[68] Zou, X.; Yao, M.; Ma, L.; Hossu, M.; Han, X.; Juzenas, P.; Chen, W. X-ray-induced nanoparticle-based photodynamic therapy of cancer. *Nanomedicine (Lond.),* **2014**, *9*(15), 2339-2351. http://dx.doi.org/10.2217/nnm.13.198 PMID: 24471504

[69] Kirakci, K.; Kubát, P.; Fejfarová, K.; Martinčík, J.; Nikl, M.; Lang, K. X-ray Inducible Luminescence and Singlet Oxygen Sensitization by an Octahedral Molybdenum Cluster Compound: A New Class of Nanoscintillators. *Inorg. Chem.,* **2016**, *55*(2), 803-809. http://dx.doi.org/10.1021/acs.inorgchem.5b02282 PMID: 26702498

[70] Kirakci, K.; Zelenka, J.; Rumlová, M.; Martinčík, J.; Nikl, M.; Ruml, T.; Lang, K. Octahedral molybdenum clusters as radiosensitizers for X-ray induced photodynamic therapy. *J. Mater. Chem. B Mater. Biol. Med.,* **2018**, *6*(26), 4301-4307. http://dx.doi.org/10.1039/C8TB00893K PMID: 32254506

[71] Hsu, C.C.; Lin, S.L.; Chang, C.A. Lanthanide-Doped Core-Shell-Shell Nanocomposite for Dual Photodynamic Therapy and Luminescence Imaging by a Single X-ray Excitation Source. *ACS Appl. Mater. Interfaces,* **2018**, *10*(9), 7859-7870. http://dx.doi.org/10.1021/acsami.8b00015 PMID: 29405703

[72] Liu, T.I.; Yang, Y.C.; Chiang, W.H.; Hung, C.K.; Tsai, Y.C.; Chiang, C.S.; Lo, C.L.; Chiu, H.C. Radiotherapy-Controllable Chemotherapy from Reactive Oxygen Species-Responsive Polymeric Nanoparticles for Effective Local Dual Modality Treatment of Malignant Tumors. *Biomacromolecules,* **2018**, *19*(9), 3825-3839. http://dx.doi.org/10.1021/acs.biomac.8b00942 PMID: 30044907

[73] Clement, S.; Chen, W.; Deng, W.; Goldys, E.M. X-ray radiation-induced and targeted photodynamic therapy with folic acid-conjugated biodegradable nanoconstructs. *Int. J. Nanomedicine,* **2018**, *13*, 3553-3570. http://dx.doi.org/10.2147/IJN.S164967 PMID: 29950835